Available online at www.sciencedirect.com
ScienceDirect
International Journal of Thermal Sciences 47 (2008) 68–75
International Journal of Thermal Sciences
www.elsevier.com/locate/ijts

Theoretical comparison of the refrigerating performances of a $CaCl_2$ impregnated composite adsorbent to those of the host silica gel

K. Daou, R.Z. Wang *, G.Z. Yang, Z.Z. Xia

Institute of Refrigeration and Cryogenics, Shanghai Jiao Tong University, Shanghai 200030, China

Received 14 May 2006; received in revised form 22 December 2006; accepted 2 January 2007

Available online 20 February 2007

Abstract

In this paper, the coefficient of performance (COP), and the specific cooling power (SCP) are theoretically evaluated for each of the two adsorbents S40 (microporous silica gel impregnated through immersion in 40% concentrated aqueous solution of calcium chloride), and S0 (the host microporous silica gel), and compared one to another. The validating data are measured on a purposely constructed single-bed basic cycle lab-scale adsorption chiller. The measured values of SCP and COP have been found far lower than those computed with the purposely developed simulation software. Those theoretical values correspond to the highest attainable ones, subject to the conditions of their evaluation. The mass ratio (MR), calculated as the ratio of SCP of S40 to that of S0, has been found to be independent of the system performance and has therefore been used to validate the model, with a rather acceptable agreement. A maximum COP value of 0.62 is predicted in the case where the composite adsorbent is used in a single-bed system with a half cycle time of 50 mm.

Keywords: Modelling; Simulation; Microporous silica gel; Composite adsorbent; Performance quantifiers

1. Introduction

Adsorption air conditioning system (ACS) is widely considered as a promising alternative to the traditional vapour compression system (VCS). It has the advantage of using environmental sound refrigerants, such as water, ammonia, and having no wearing parts. Even more importantly, it can be driven directly by thermal energy, thereby offering the possibility of utilising waste heat, which can also come free.

The major drawbacks hindering its competitiveness against the environmental unfriendly refrigerant vapour compression system are its bulkiness and its low operating efficiency. Those drawbacks can be addressed by designing heat and mass transfer enhanced adsorbers as well as through heat and mass recovery and other regenerative cycles [1–4]. These very same problems can be tackled by utilising low temperature energy free sources, such as exhausted industrial coolants, solar energy, geothermal energy etc., as driving heat. Their harnessing in energising the ACS can help boost dramatically the competitiveness of that technology, as it obviates the needs for excessive concerns about its rather poor operating efficiency.

Utilisation of those energy sources, however, requires the use of adsorbents that can be regenerated at low temperatures attainable in solar collectors or available in exhausted low temperature coolants. Silica gel is largely used as adsorbent with the water as refrigerant, when it comes to utilise the low temperature waste heats in adsorption refrigeration and air conditioning. But its adsorption capacity hardly exceeds 40% of its own weight. Therefore there is a need for developing new adsorbents of high adsorption capacity and capable of being regenerated at low temperatures. The research on so called Selective water sorbents, which are developed by impregnating some hydrophilic or hydrophobic porous materials with hygroscopic salts, was initiated and are still ongoing in the Boreskov Institute of Catalysis [5–8]. A theoretical cooling COP of 0.7 to 0.8 have been predicted and a maximum cooling COP of 0.6 have been experimentally obtained from system using those adsorbents and driven by low temperature heat sources (less than 100 °C) [8]. M.Z.I. Khan et al., on their part [9], investigated theoretically and experimentally a two-stage innovative chiller

* Corresponding author. Tel.: +86 21 62933838; fax: +86 21 62933250.
E-mail address: rzwang@sjtu.edu.cn (R.Z. Wang).

1290-0729/$ – see front matter
doi:10.1016/j.ijthermalsci.2007.01.003

Nomenclature

k	thermal conductivity coefficient	$W\,m^{-1}\,K^{-1}$
ΔH	heat of adsorption (Resp. desorption)	J
T	temperature	K
Q	quantity of heat exchanged	J
COP	coefficient of performance	
W	adsorption level	$kg\,kg^{-1}$
W_0	saturation adsorption capacity	$kg\,kg^{-1}$
SCP	specific cooling power	$W\,kg^{-1}$
M	mass of adsorbent used	kg
L, h_{lg}	latent heat of evaporation, heat of vaporisation	$J\,kg^{-1}$
C_p	heat capacity at constant pressure	$J\,kg^{-1}\,K^{-1}$
C_f	heat capacity of heat exchanger fluid	$J\,kg^{-1}\,K^{-1}$
$\dot{m}_f$	mass flow rate of heat exchanger fluid	$kg\,s^{-1}$
U	global coefficient of heat transfer of the bed	$J\,kg^{-1}$
R	specific Universal Gas Constant	$J\,kg^{-1}\,K^{-1}$
P	pressure	Pa
$t_{1/2}$	half cycle time	s
A	area of adsorber heat exchanger	m^2

Subscripts

comp	composite adsorbent
as	adsorbent
ex	metal of adsorber heat exchanger
cont	container
d	desorption
c	condensation
cps	supplied during condensation proper
dp	desorption proper (resp. adsorption proper)
v	vapour
w	water, wall
t	tube (copper tube)
a	adsorbent layer
max	maximum
min	minimum
e	evaporator

Prefix

exp	experimental
th	theoretical

using silica gel and water as working couple and driven by waste heat between 50 and 70 °C. The authors showed that the performance of the system is influenced by the overall heat conductance of the adsorber and the condenser. In addition, the use of re-heat in the system led to the improvement of COP by 36% while, on the contrary, the SCP suffered a loss of 4% in comparison with the conventional two-stage chiller. A COP value slightly higher than 0.6 was obtained for an amount of silica gel of 7 kg charged in the adsorber. Shanghai Jiao Tong University is also actively engaged in research activity regarding salt impregnated composite adsorbents [10]. B.B. Saha et al. [11] carried out an analytical study on an innovative three-bed adsorption chiller and showed that its performance characteristics – the cooling capacity and the coefficient of performance – were strongly influenced by the thermal conductances of the adsorber/disrober, the evaporator and the condenser. A particularly strong dependence was found between those performance characteristics and the adsorbent-to-metal thermal capacitance ratio. The modelled chiller was driven by waste heat at the temperature between 60 and 95 °C with a cooling temperature of 30 °C. B.B. Saha et al. [12] modelled an electro-adsorption chiller, which was a hybrid system modelling the isotherm and the dynamic behaviour of water adsorption on silica gel as well as the properties of thermoelectric elements. The authors obtained a COP of up to 0.81 from the two potentially low COP systems amalgamated. The system was shown to be superior to all others alternative systems used in cooling computer CPU.

In this article, the theoretical performances of a composite adsorbent obtained by inserting calcium chloride into the pores spaces of microporous silica gel are compared to those yielded in similar conditions by the host silica gel. These theoretical results are, in turn, compared to the experimental ones for both adsorbents. The data computed are meant to yield the highest values attainable of the quantities evaluated, subject to the system performance and the operating conditions. Since the experimental system is not designed for enhance heat and mass transfer, which would have brought theoretical values closer experimental ones, the theoretical are expected to be higher than the experimental. The mass ratio, however, which is defined as the ratio of the specific cooling power (SCP) of the composite adsorbent to that of the host silica gel, is expected to be independent of system performance. Agreement between the theoretical and experimental data of that quantity will serve validate the model developed.

2. Description of the impregnation process

The impregnation of the calcium chloride into the pore volumes of the host silica gel comprises mainly the preparation of the aqueous of calcium and the immersion of the silica gel in that solution.

The preparation of aqueous solution of silica gel has consisted of putting 40% of calcium chloride in relation to the total weight of water and the calcium being used. The solution was then kept under ambient temperature (which was about 27 °C for this sample) for two hours and stirred up from time to time with the purpose of facilitating and accelerating the dissolution process, and preventing crystallisation. Grains of microporous host silica gel were immersed thereafter in the prepared solution and kept therein for twelve hours in order to allow the salt solution to penetrate and fill all the pore volumes. The soaked silica gel was then poured into a sieve-like vessel to filter the

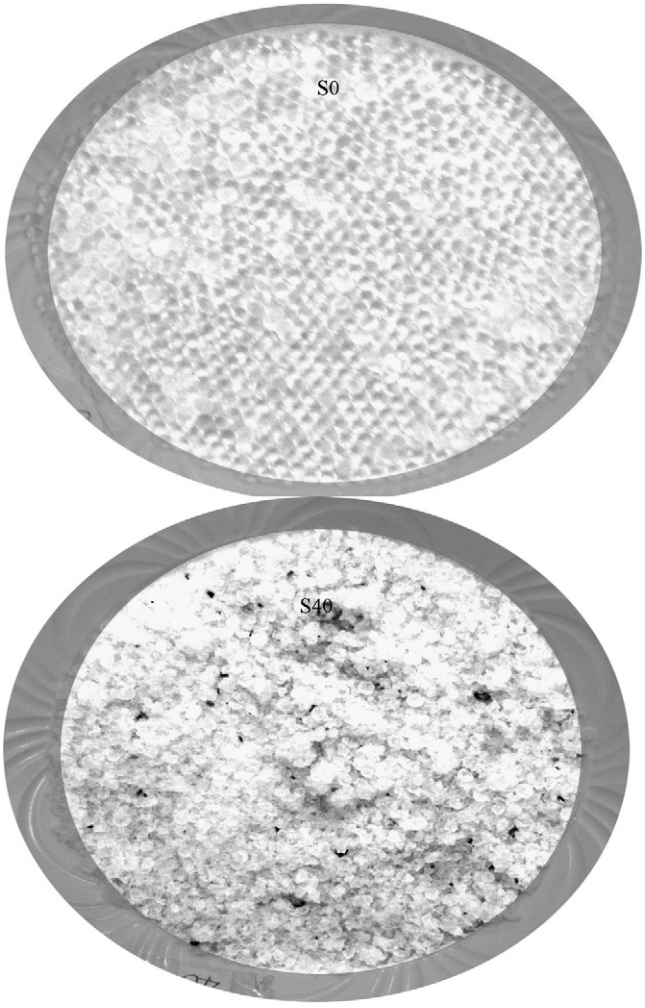

Fig. 1. Textural aspect of S0 and S40.

poorly concentrated aqueous solution out of it. The samples were then laid and scattered afterwards on plastic trays, which were placed on shelves inside a thermostatic-humidistat chamber where they were dried under a temperature of 80 °C. This thermostatic chamber allows choosing and keeping constant both the temperature and the humidity inside.

During the drying process, the samples were being taken out and weighed from to time until their weight losses were found negligibly small. An electronic scale having an accuracy of ±0.01 g was used for the weighting.

The contents of $CaCl_2$ in the anhydrous samples were calculated and designated in terms of percentage with respect to the total weight of the host silica gel and the calcium chloride used. Fig. 1 presents textural aspect of the parent silica gel alongside that of the composite adsorbent obtained, after they have undergone a certain number of cycles. A microscopic image taken of the composite adsorbent has shown a very fragmented structure (Fig. 2). This fragmentation is an unwelcome outcome as it contributes to reducing, somewhat, the adsorption capacity following the destruction of the network of linked pore volumes.

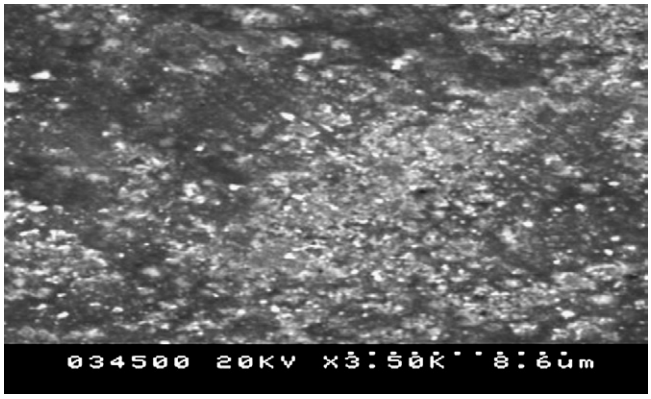

Fig. 2. Electronic microscopic image of S40.

3. Derivation of the governing equations

3.1. Conditions and assumptions

For the purpose of modelling the system, the following assumptions are made:

- The vapour of refrigerant water is considered as behaving like a perfect gas.
- The thermal capacities of metal, adsorbent and thermal fluids are assumed constant.
- An average specific heat capacity, $C_{pv} = 1.9045$ kJ/kg K, of saturated water stream was used over the temperature range spanning 0–90 °C.
- The adsorption level is considered as reaching the equilibrium state at the temperature and pressure considered.
- The half cycle time has been set to 2 hours to take into account the performance of the experimental setup whose data are used to validate the model.

The setup has not been designed for enhanced heat and mass transfer. Therefore, it is expected to yield lower experimental performance and lengthier cycle time than for a heat and mass transfer enhanced system. Nevertheless, since it is used for comparison purpose, it can be assumed that its poor performance will affect the two adsorbents in the same way and to the same extent. Consequently, the mass ratio, MR, defined as the ratio of the SCP of the composite adsorbent to that of the pure silica gel, can be taken as a system performance independent quantity.

3.2. Governing equations

Since the composite adsorbent is new and no established equation specifically governing its adsorption behaviour exists, the Dubinin–Astakhov equation (1) is used, with its coefficients D, n, and w_0 calculated by applying the least square regression fitting.

$$W = W_0 \exp\left[-D\left(T \ln \frac{P_S}{P}\right)^n\right] \tag{1}$$

The calculated D–A equation coefficients, for the two adsorbents, are tabulated in Table 1.

Table 1
Fitting results to D–A equation

Sample	n	w_0	D	δ (%)
S0	1.7	0.35	6×10^{-6}	1.2
S40	1.65	0.68	15.6×10^{-6}	2.06

Table 2
Regression coefficients of the latent heat of vaporisation of water

Temperature range (K)	C_1	C_2	Number of data	Maximum deviation (%)
273.15–373.15	3167.5966	−2.4322	100	0.14

In very much the same way, a linear correlation is established between the heat of vaporisation and the saturation temperature and presented as Eq. (2):

$$h_{\mathrm{lg}} = C_1 + C_2 T \tag{2}$$

The data extracted from the reference [13] are fitted to Eq. (2) through the least-square regression. The calculated values of the constants C_1 and C_2 are tabulated in Table 2.

Application of the Clausius–Clapeyron equation assists to establish a relation between the saturated refrigerant vapour pressure and its temperature. The sought relation is obtained in the form of relation (3).

$$\ln P_{\mathrm{s}} = b - m\frac{1}{T} \tag{3}$$

Eq. (1) can be written in the form of Eq. (4) as follow:

$$\frac{W}{W_0} = \exp\left(-DT^n\left(\ln\frac{P_{\mathrm{s}}}{P}\right)^n\right) \tag{4}$$

Taking the logarithms of the two members of that equation and after separation of pressure terms from the others, one obtains Eq. (5).

$$\ln P_{\mathrm{s}} - \ln P = \frac{1}{T}\left(-\frac{1}{D}\ln\frac{W}{W_0}\right)^{1/n} \tag{5}$$

Substituting into Eq. (5) the refrigerant's saturated pressure, already given in Eqs. (3), (5) can be transformed into Eq. (6) as follow:

$$\ln P = b - m\frac{1}{T} - \frac{1}{T}\left(-\frac{1}{D}\ln\frac{W}{W_0}\right)^{1/n} \tag{6}$$

After some arrangements, the sought relation linking the pressure of the refrigerant, the temperature of the adsorbent bed and the adsorption level is found in the form of Eq. (7) presented below.

$$\ln P = b - \frac{1}{T}\left(m + \frac{1}{D^{1/n}}\left(-\ln\frac{W}{W_0}\right)^{1/n}\right) \tag{7}$$

where, b and m are constants of integration, and T is the temperature of refrigerant vapour. Data extracted from the reference [13] were fitted to Eq. (3) by the least-square regression method. Thus, the numerical values of the coefficient b and m are determined and tabulated in Table 3.

Table 3
Calculated coefficients of water vapour saturated curve

Temperature range (K)	b	m	Number of data	Maximum relative error (%)
273.15–373.15	25.5127	−5206.3276	100	3.83

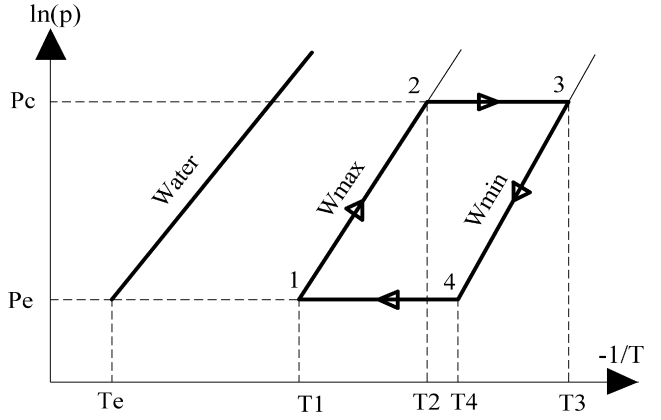

Fig. 3. Theoretical classical basic cycle in Clapeyron's ($\ln P$, $1/T$) diagram.

The pressure in the adsorbent bed can be obtained by combining Eqs. (1) and (3). After some transformations, the relation liking the adsorbent bed pressure to both the temperature of refrigerant vapour and the adsorption level is expressed by Eq. (8).

$$\ln P = b - \frac{1}{T}\left(m + \frac{1}{D^{1/n}}\left(-\ln\frac{W}{W_0}\right)^{1/n}\right) \tag{8}$$

The isosteric (constant adsorption level) heat of adsorption can be readily derived from the Clapeyron–Clausius equation.

$$\left(\frac{\partial P}{\partial T}\right)_{\mathrm{w}} = \frac{\Delta H_{\mathrm{va}}}{T(v_{\mathrm{v}} - v_{\mathrm{a}})} \tag{9}$$

The specific volume of the adsorbed phase (considered at liquid phase) is negligible in respect to that of vapour phase and, and therefore, it can be neglected in this equation. Hence, Eq. (9) can be put in the form of Eq. (10).

$$\left(\frac{\partial P}{\partial T}\right)_{\mathrm{w}} = \frac{\Delta H_{\mathrm{va}}}{T v_{\mathrm{v}}} = \frac{\Delta H_{\mathrm{va}}}{RT^2/P} \tag{10}$$

which, after the transformations (11) and (12), and after substituting the derivation of the pressure P with respect to the inverse of temperature in the equation, as expressed in Eq. (8), can be put into the form of Eq. (13).

$$\frac{\partial P/P}{\partial T/T^2} = \frac{\Delta H_{\mathrm{va}}}{R} = \frac{\mathrm{d}(\ln(P))}{\mathrm{d}(1/T)} \tag{11}$$

hence,

$$\Delta H_{\mathrm{va}} = -R\frac{\mathrm{d}(\ln(P))}{\mathrm{d}(1/T)} \tag{12}$$

$$\frac{\partial(\ln P)}{\partial(1/T)} = m + \frac{1}{D^{1/n}}\left(-\ln\frac{W}{W_0}\right)^{1/n} = \frac{\Delta H_{\mathrm{va}}}{R} \tag{13}$$

Table 4
Thermal capacity of the adsorber heat exchanger

Components	Mass (kg)	Material	C_p (J/(kg K))	Thermal capacity (J/K)
Fins	0.28	aluminium	902	251.32
Tubes	1.45	copper	386	560.26
Container + flange	12.00	steel	465	5580.23
Total	13.73			6391.81

Thus, after some arrangements, the isosteric heat of adsorption (resp. desorption) can be put into the form (14).

$$\Delta H_{va}(W) = Rm + R\frac{1}{D^{1/n}}\left(-\ln\frac{W}{W_0}\right)^{1/n} \tag{14}$$

where R represents the specific universal gas constant of the refrigerant vapour (water vapour). In accordance with the above Clapeyron's diagram (Fig. 3), the energy conservation equation (15) expresses the heat input brought in the system by the heating hot water.

$$\begin{aligned} Q_{input} &= \left[M_{ex}C_{pex} + M_{as}(C_{Pas} + C_{Pw}W_{max})\right](T_2 - T_1) \\ &\quad + Q_{cps} + Q_{dp} \\ &= \int_0^{t_{1/2}} \left(\dot{m}_f C_{pf}\varepsilon(T_{hotwin} - T_{hotwout})\right) \mathrm{d}t \end{aligned} \tag{15}$$

In Eq. (15), the first term in the left-hand side represents the sensible heat spent to heat the adsorbent bed (adsorbent plus metal) from T_1 to T_2 (isosteric heating). The second term Q_{cps} and the third term Q_{dp} are the sensible heat and the latent heat of desorption respectively. C_{Pas} designates the specific thermal capacity of the adsorbent, C_{Pw} represents the same quantity for the adsorbed state of the refrigerant (state taken as that of water liquid), and W_{max} denotes the maximum adsorption level, which is different from the saturated adsorption capacity, W_0. The symbol M_{ex} sands for the total mass of heat exchanger metal, which includes the fins, the heat exchanger copper tubes and the plate serving as support for mounting the adsorber in the main frame. The heat capacities of all constituent components of the adsorber heat exchanger are calculated and tabulated in Table 4. The total heat capacity is calculated according to Eq. (16) and the result is also presented in the same table.

$$M_{ex}C_{pex} = M_{fin}C_{fin} + M_{tube}C_{tube} + M_{cont}C_{cont} \tag{16}$$

where M_{cont}, and C_{cont} denote respectively the mass and the thermal capacity of the container plus the fixing flange; and M_{ex} and C_{ex} represent the same quantities for the whole adsorber heat exchanger.

The sensible heat supplied Q_{cps} to heat the adsorbent bed from T_2 to T_3, can be expressed by Eq. (17) presented below:

$$\begin{aligned} Q_{cps} &= (M_{ex}C_{pex} + M_{as}C_{pas})(T_3 - T_2) \\ &\quad + MC_{pv}\int_{T_2}^{T_3} W(T)\,\mathrm{d}T \end{aligned} \tag{17}$$

Table 5
Characteristics of the adsorbent bed

Characteristics	Value and unit
Surface area, A	1.4206 m^2
U (with S40 charged)	8.257 $W\,m^{-2}\,K^{-1}$
U (with silica gel charged)	3.846 $W\,m^{-2}\,K^{-1}$

The heat of desorption proper, Q_{dp}, presented in Eq. (15), can be calculated by Eq. (18) as follow:

$$Q_{dp} = M\int_{W_{min}}^{W_{max}} \Delta H_{av}\,\mathrm{d}W \tag{18}$$

The bed efficiency can be calculate by Eq. (19)

$$\varepsilon = 1 - \mathrm{e}^{-UA/(\dot{m}_f C_{pf})} \tag{19}$$

In this relation U is the overall heat transfer coefficient of the bed and is calculated by Eq. (20).

$$U = \left(\frac{1}{R_w} + \frac{1}{R_t} + \frac{1}{R_a}\right)^{-1} \tag{20}$$

where R_w, is the thermal resistance to the convective heat transfer between the hot water and the tube internal wall; R_t is the thermal resistance due to the tube and its value is determined by the thermal conductivity and the thickness of the tube; and R_a, is the thermal resistance offered by the bulk of the of adsorbent and is determined in magnitude by the packed adsorbent effective thermal conductivity. Here, the thermal resistances at the interfaces of the adsorbent and the adsorber heat exchanger copper tubes as well as the fins have not been taken into account. The calculated heat transfer characteristics of the adsorbent bed are shown in Table 5.

Finally, when the desorption temperature is known or assumed, the hot water outlet temperature can be calculated by Eq. (21), since its inlet temperature and the adsorbent bed heat transfer characteristics are known.

$$\frac{T_{hotwout} - T_d}{T_{hotwin} - T_d} = \mathrm{e}^{-UA/(\dot{m}_f C_{pf})} \tag{21}$$

where $T_{hotwout}$ is the outlet temperature of the hot water and T_{hotwin} while denotes its inlet temperature. T_d represents the temperature of the adsorbent and the adsorber heat exchanger taken as lump object and considered to be at uniform temperature.

The flowrate of the hot water considered in this calculation is the same as that used during the experiments, and is equal to $\dot{m}_f = 0.0487$ kg/s. The specific thermal capacity of water is assumed constant and its value is given as $C_f = 4180\ J\,kg^{-1}\,K^{-1}$.

The evaporator heat gain which constitutes the heat withdrawn from the chilled heat exchange fluid, producing the cooling effect, is equal to the latent heat of evaporation of the cycled refrigerant minus the sensible heat required to cool the liquid refrigerant from the condensation temperature down to the evaporating temperature, as in Eq. (22)

$$Q_e = M(W_{max} - W_{min})\left[L(T_e) - \int_{T_e}^{T_c} C_{pw}\,\mathrm{d}T\right] \tag{22}$$

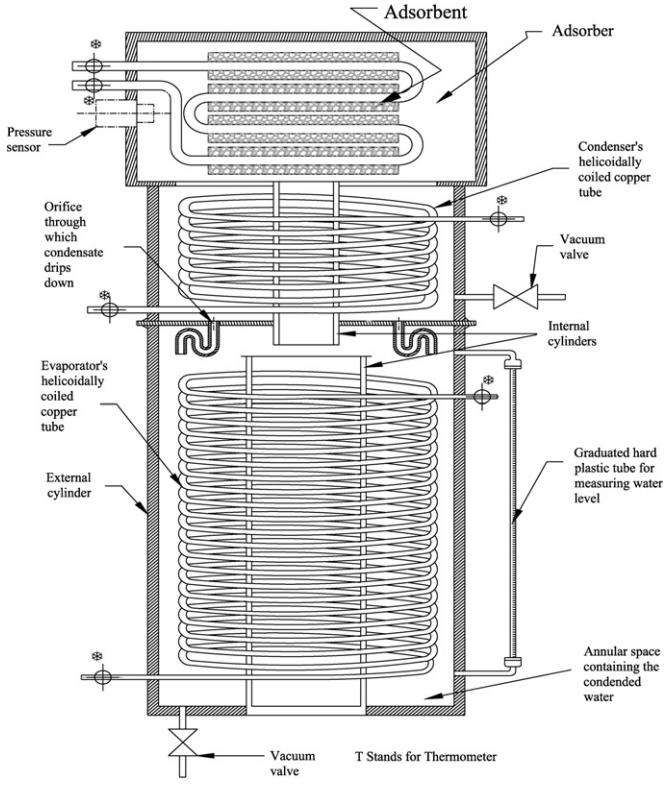

Fig. 4. Experimental rig with the different instruments used for measurement.

The specific cooling power (SCP) is defined as cooling power yielded by the evaporator per unit mass of adsorbent and over the half cycle time of adsorption operation.

$$SCP = \frac{Q_e}{Mt_{1/2}} \tag{23}$$

where $t_{1/2}$ designates the half cycle time and M represents the amount (mass) of adsorbent used.

The coefficient of performance is calculated as the ratio of the cooling effect received in the evaporator to the total heat supplied to the adsorbent bed during the desorption of the refrigerant from the adsorbent.

$$COP = \frac{Q_e}{Q_{input}} \tag{24}$$

The mass ratio is calculated by dividing the SCP of the composite by the SCP of silica gel.

$$MR = \frac{(SCP)_{comp}}{(SCP)_{silica}} \tag{25}$$

where $(SCP)_{comp}$ designates the specific cooling power of the composite adsorbent S40 and $(SCP)_{silica}$ represents that of the pure silica gel S0, while MR stands for mass ratio.

A PC based software was developed in Microsoft Visual C++, and used to simulate numerically the model thus developed. The following section deals with the generation of experimental data and their comparison with the theoretical ones yielded by the software.

4. Experimental data produced and confronted with the theoretical ones

4.1. Description of the lab-scale adsorptive chiller

The system is a small lab-scale, single-bed, basic adsorption chiller system operating without any valves on its refrigerant circuit. The condenser and the evaporator are made of helicoidally coiled copper tubes, placed inside the evacuated annular space formed by three coaxial cylinders (Fig. 4). The adsorber (Fig. 5) is constituted of copper tubes onto which are appended fins made in aluminium. The geometrical and material characteristics of the container, the heat exchange copper tubes and the fixing flange are listed in Tables 6 and 7. The

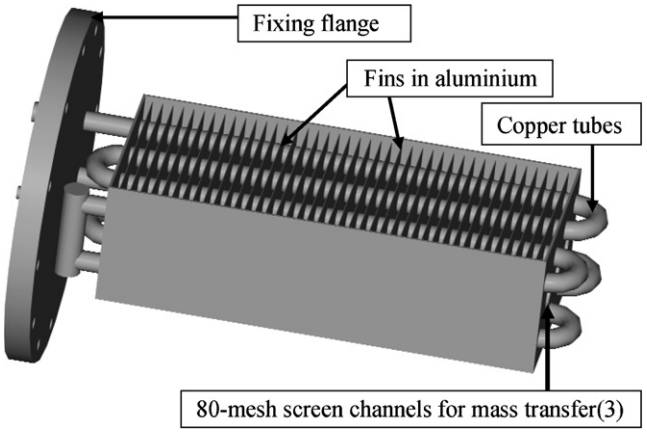

Fig. 5. Perspective drawing of the adsorber heat exchanger.

Table 6
Adsorber design parameters

Tubes	material	copper
	number	8
	diameter	16 mm
	length	337 mm
	thickness	1.2 mm
Adsorber	material	steel
	height	102 mm
	width	150 mm
	thickness	2 mm
Fins	material	aluminium
	thickness	0.16 mm
	number	42
	spacing	8 mm

Table 7
Thermophysical characteristics of the involved materials

Steel	Heat conductivity coefficient (W/m K)	49.8
	Specific thermal capacity (J/kg °C)	465
	Density (kg/m^3)	7840
Aluminium	Heat conductivity coefficient (w/m K)	236
	Specific thermal capacity (J/kg K)	902
	Density (kg/m^3)	2710
Copper	Heat conductivity coefficient (w/m K)	398
	Specific thermal capacity (J/kg K)	386
	Density (kg/m^3)	8930

amounts of adsorbent charged in the bed were 1.2 kg for the pure silica gel and 0.8 kg for the composite adsorbent.

4.2. Functional description of the lab-scale adsorptive chiller

For the sake of modelling, the lab-scale chiller is considered to be functioning in four phases (Fig. 3) namely the isosteric heating–pressurisation, 1–2, the isobaric heating–condensation, 2–3, the isosteric cooling–depressurisation, 3–4, and the isobaric cooling–adsorption, 4–1. Owing to the geometrical configuration of the setup – marked by the absence of any regulating valves – the system is actually operated by combining the first two processes into one heating–desorption–condensation phase and the last two into another, which is the cooling–adsorption–evaporation phase. During the heating–desorption–condensation phase, the hot water is circulated in the adsorber, the adsorbent is therefore heated and the water refrigerant, previously adsorbed, is consequently expelled from it in form of vapour. The vapours thus released get into contact with the cooled external surface of copper tube, condense thereon, and drip down into the evaporator through two holes made for that purpose. During the second phase, the adsorbent bed is cooled down, causing the previously desorbed refrigerant vapour to be adsorbed anew. This adsorption causes the evaporation of the liquid refrigerant inside the evaporator producing the cooling effect. The cold thus produced is absorbed by the chilled water circulated in the evaporator.

The temperature of water circulated in the condenser was maintained around 30 °C during experiments, while the chilled water temperature could be controlled in a wide range spanning 8–20 °C, depending upon application demands, the desorption temperature was set to 80 °C.

4.3. Comparison of theoretical and experimental results and discussions

In Figs. 6–8, the computed SCP and MR, for the two adsorbents are compared with experimental ones, at the isobaric adsorption corresponding to the saturated temperatures 8.4 °C, 10 °C, and 15 °C respectively. As illustrated by the above mentioned figures, both the computed and experimental SCP values of S40 are much higher than those of S0. It is also seen that the experimental data of MR as well as theoretical ones, increase monotonically, fluctuating within a narrow interval of values

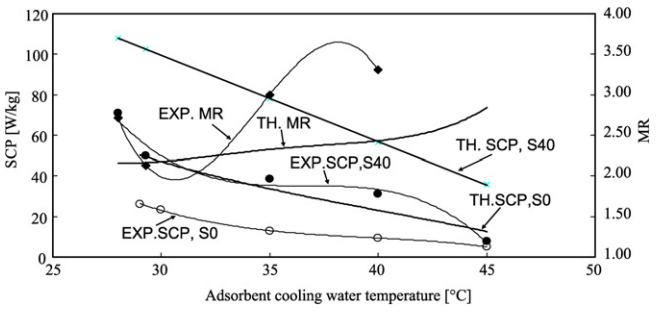

Fig. 6. Experimental and theoretical SCP and MR at CHEXF temperature of 8.4 °C.

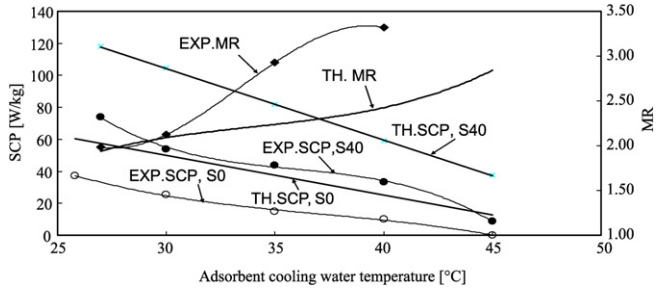

Fig. 7. Experimental and theoretical SCP and MR at CHEXF temperature of 10 °C.

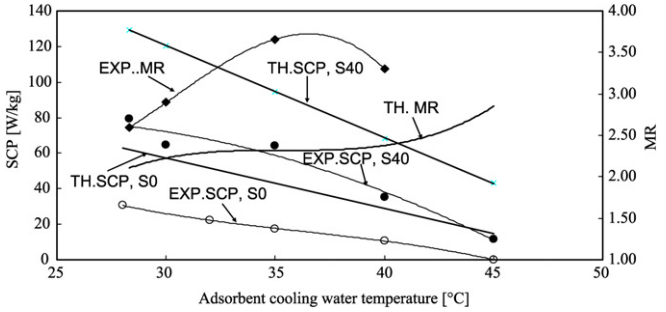

Fig. 8. Experimental and theoretical SCP and MR at CHEXF temperature of 15 °C.

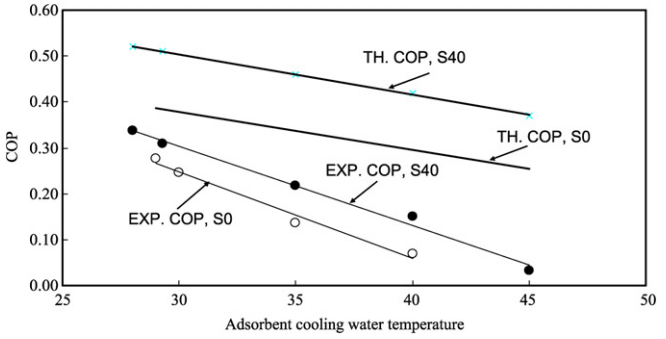

Fig. 9. Compared theoretical and experimental COP of S0 and S40 at CHEXF temperature of 8.4 °C.

ranging from 2 to 3.5. The amplitude of that fluctuation indicates that the theoretical and experimental data are in a fairly good agreement.

As to the computed values of COP, it is seen in Figs. 9–11 that, on the one hand, both theoretical and experimental COPs of the composite adsorbent are found to be much higher than their corresponding values yielded by the pure silica gel. On the other hand, the theoretical results obtained with either adsorbent are also much higher than the experimental ones. It can be concluded from those results that, in addition to enabling utilisation of lower temperature waste heats, the composite adsorbent brings about improvement of system operating efficiency. The rather low experimental COP stems from the fact that the lab-scale chiller system used in carrying out the testing has not been designed for enhanced heat and mass transfer. The use of multi-bed adsorbers, the better design thereof, and the implementation of heat and mass recovery cycles can contribute to improving significantly the experimental values of COP, bring-

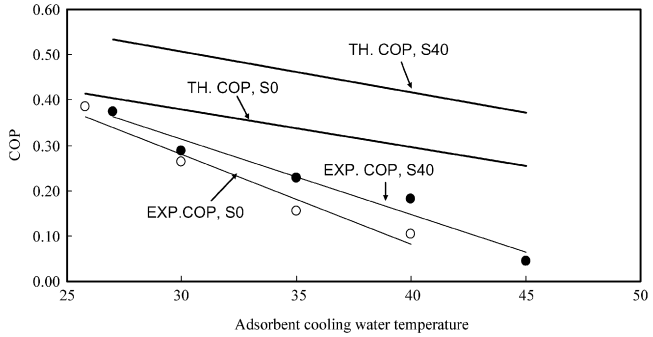

Fig. 10. Compared theoretical and experimental COP of S0 and S40 at CHEXF temperature of 10 °C.

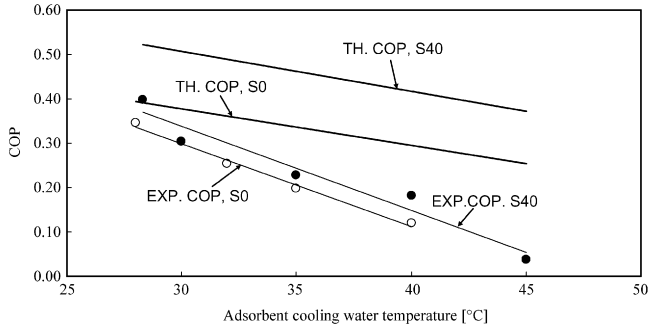

Fig. 11. Compared theoretical and experimental COP of S0 and S40 at CHEXF temperature of 15 °C.

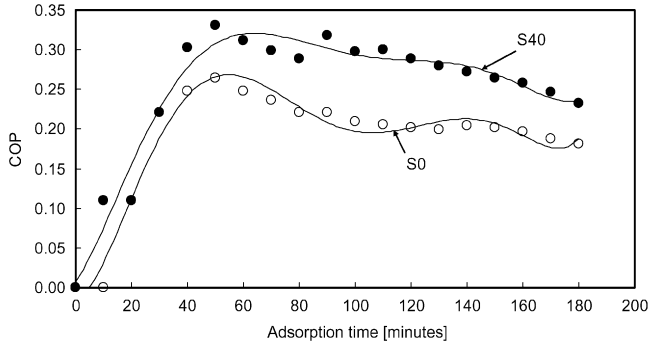

Fig. 12. Variation of the COP of the two adsorbents with adsorption time.

ing them up closer to the theoretical ones. The half cycle time adopted here has been chosen long so as to take the rather poor performance of system into account. Experimentally the highest COP of the system was reached at the half cycle time of about 50 minutes (see Fig. 12). Theoretically, for the same half cycle time, a maximum COP of 0.62 has been predicted using the software purposely developed to simulate the model developed.

5. Conclusion

This comparative theoretical study has shown that the mass ratio (MR) is, in all operating conditions, higher than 2. Consequently, the quantity of adsorbent needed to produce a given cooling power can be reduced as much as twice, if the composite adsorbent is used in lieu of the host pure silica gel. The impregnation operation has been also shown to improve the coefficient of performance (COP), though to a far lesser extent than the SCP.

In the case where the half cycle time is reduced to the optimal value of 50 minutes, a maximum COP value of 0.62 is predicted if the composite adsorbent is used in a single bed system.

References

[1] D.C. Wang, Z.Z. Xia, H. Zhai, J.Y. Wu, R.Z. Wang, H. Zhai, W.D. Dou, Study of a novel silica gel-water adsorption chiller: Part I. Design and performance prediction, International Journal of Refrigeration 28 (2005) 1073–1083.

[2] D.C. Wang, J.Y. Wu, Z.Z. Xia, H. Zhai, R.Z. Wang, W.D. Dou, Study of a novel silica gel-water adsorption chiller: Part II. Experimental study, International Journal of Refrigeration 28 (2005) 1084–1091.

[3] Y.L. Liu, R.Z. Wang, Z.Z. Xia, Experimental study on a continuous adsorption chiller with novel design, International Journal of Refrigeration 28 (2005) 218–230.

[4] B.B. Saha, S. Koyama, T. Kashiwagi, A. Akisawa, K.C. Ng, H.T. Chua, Waste heat driven dual-mode multistage, multi-bed regenerative adsorption system, International Journal of Refrigeration 26 (2003) 749–757.

[5] L.G. Gordeeva, G. Restuccia, A. Freni, Yu.I. Aristov, Water sorption on composites “LiBr in a porous carbon”, Fuel Processing Technology 79 (2002) 225–231.

[6] Yu.I. Aristov, Selective water sorbents (SWSs): Design of sorption properties, in: International Sorption Heat Pump Conference, Denver, CO, USA, June 22–24, 2005, ISHPC-069-2005.

[7] A. Freni, F. Russo, S. Vasta, M. Tokarev, Yu.I. Aristov, G. Restuccia, An advanced solid sorption chiller using SWS-1L, Applied Thermal Engineering, in press, Corrected Proof, Available online 30 September 2005.

[8] G. Restuccia, A. Freni, S. Vasta, Yu. Aristov, Selective water sorbents for sorption chiller: Experimental results and modeling, International Journal of Refrigeration 27 (2004) 284–293.

[9] M.Z.I. Khan, K.C.A. Alam, B.B. Saha, Y. Hamamoto, A. Akisawa, T. Kashiwagi, Parametric study of a two-stage adsorption chiller using reheat – The effect of overall thermal conductance and adsorbent mass on system performance, International Journal of Thermal Sciences 45 (2006) 511–519.

[10] K. Daou, R.Z. Wang, Z.Z. Xia, Development of a new synthesized adsorbent for refrigeration and air conditioning applications, Applied Thermal Engineering 26 (2006) 56–65.

[11] B.B. Saha, A. Chakraborty, S. Koyama, K.C. Ng, M.A. Sai, Performance modelling of an electro-adsorption chiller, Philosophical Magazine 86 (2006) 3613–3632.

[12] B.B. Saha, I.I. El-Sharkawy, S. Koyama, J.B. Lee, K. Kuwahara, Waste heat driven multi-bed adsorption chiller: heat exchangers overall thermal conductance on chiller performance, Heat Transfer Engineering 28 (2006) 80–87.

[13] E. Schmidt, Properties of Water and Steam in SI-Units, Third enlarged printing, Springer, Berlin, 1991, Edited by Urich Grigull.